

Discretization Methods for Solids Undergoing Finite Deformations

Peter Wriggers

Abstract Finite element methods for solving engineering problems are used since decades in industrial applications. This market is still growing and the underlying methodologies, formulations, and algorithms seem to be settled. But still there are open questions and problems when applying the finite element method to situations where finite strains occur. Another problem area is the incorporation of constraints into the formulations, such as incompressibility, contact, and directional constraints needed to formulate anisotropic material behavior. In this section, we present the basic continuum formulation and different discretization techniques that can be used to overcome the problems mentioned above. Additionally, a set of test problems is presented that can be applied to test new finite element formulations.

1 Basic Equations of Continuum Mechanics

A short summary of continuum mechanics is provided in order to be able to formulate the basis for finite element discretizations of finite strain problems. This summary includes kinematical relations, balance laws with their weak forms, and a selection of constitutive equations.

The kinematical relations and associated strain measures used within discretizations are described. Variational formulations are derived based on balance laws that are basis for nonlinear finite element methods. Isotropic hyperelastic material behavior is discussed as an example for nonlinear constitutive equations. Furthermore, all relations will be provided for small strains, leading to the well-known linear relations.

Since this chapter is devoted to nonlinear finite element formulations the underlying theory of continuum mechanics cannot be treated in depths. For this we refer to standard books, e.g., Truesdell and Toupin (1960), Truesdell and Noll (1965), Eringen (1967), Malvern (1969), Becker and Bürger (1975),

P. Wriggers (✉)

Institute of Continuum Mechanics, Gottfried Wilhelm Leibniz Universität,
Hannover, Germany
e-mail: wriggers@ikm.uni-hannover.de

Altenbach and Altenbach (1994), Chadwick (1999) or Holzapfel (2000), Ogden (1984), Marsden and Hughes (1983) and Ciarlet (1988) which give background in continuum theory and its mathematical background.

1.1 Kinematics

The kinematical relations concern in continuum mechanics the description of the deformation and motion of a body. They are basis for the derivation of strain measures.

Motion, deformation gradient The motion of a body can be described with respect to the initial configuration or the current configuration of a body. In general, the motion of body B is given as a series of configurations

$$\mathbf{x} = \varphi(\mathbf{X}, t), \quad (1)$$

where \mathbf{X} is the position vector defining a point in the initial configuration B . The map $\varphi(\mathbf{X}, t)$ maps this point to the current/spatial configuration, described by the position vector \mathbf{x} . The position vector can be written in component form as $\mathbf{X} = X_A \mathbf{E}_A$ where \mathbf{E}_A defines an orthogonal base system in the initial configuration. Hence, one can write (1) in terms of components of the vectors as $x_i = \varphi_i(X_A, t)$. Using, instead of \mathbf{X} , the spatial coordinates \mathbf{x} leads to the called current, spatial or Eulerian description of motion.¹

By introducing a displacement vector $\mathbf{u}(\mathbf{X}, t)$ as difference between the position vectors of current and initial configuration

$$\mathbf{u}(\mathbf{X}, t) = \varphi(\mathbf{X}, t) - \mathbf{X} \quad (2)$$

the current coordinates $\mathbf{x} = \varphi(\mathbf{X}, t)$ can be expressed by $\mathbf{x} = \mathbf{X} + \mathbf{u}(\mathbf{X}, t)$.

Local deformations can be investigated by introducing the deformation gradient \mathbf{F} . The deformation gradient maps a material line element of the initial configuration $d\mathbf{X}$ in B , to a line element $d\mathbf{x}$ of the current configuration $\varphi(B)$.

$$d\mathbf{x} = \mathbf{F} d\mathbf{X}. \quad (3)$$

The components form of the deformation gradient can be written as

$$\mathbf{F} = \text{Grad } \varphi(\mathbf{X}, t) = \frac{\partial x_i}{\partial X_A} \mathbf{e}_i \otimes \mathbf{E}_A. \quad (4)$$

The connection within B during the deformation process the mapping (3) has to be one-to-one which excludes singularity of \mathbf{F} and further to exclude self-penetration one obtains the restriction

¹Small letters are used for indices of vectors and tensors which are related to the basis \mathbf{e}_i of the current or spatial configuration. The quantities x_i are the spatial coordinates of X .

$$J = \det \mathbf{F} > 0, \quad (5)$$

where J defines the Jacobi determinant. Hence \mathbf{F} is regular and the inverse \mathbf{F}^{-1} exists.

With the deformation gradient the transformation of surface area elements between B and $\varphi(B)$ can be expressed by the formula of Nanson,

$$\mathbf{d}\mathbf{a} = \mathbf{n} da = J \mathbf{F}^{-T} \mathbf{N} dA = J \mathbf{F}^{-T} \mathbf{d}\mathbf{A}. \quad (6)$$

In this equation \mathbf{n} is the normal vector of the surface of the deformed body $\varphi(B)$ and \mathbf{N} is the normal vector in the initial configuration B . J is the Jacobi determinant and da and dA are the area elements of the associated configurations, respectively.

The transformation between volume elements of the initial and current configuration is given by

$$dv = J dV. \quad (7)$$

The deformation gradient can be written in terms of the displacements as

$$\mathbf{F} = \text{Grad} [\mathbf{X} + \mathbf{u}(\mathbf{X}, t)] = \mathbf{1} + \text{Grad} \mathbf{u} = \mathbf{1} + \mathbf{H}. \quad (8)$$

with the displacement gradient $\mathbf{H} = \text{Grad} \mathbf{u}$.

Strain measures Different strain measures are introduced that are used in forthcoming formulations. The Green-Lagrange strain tensor is referred to the initial configuration B . It is defined by

$$\mathbf{E} = \frac{1}{2} (\mathbf{F}^T \mathbf{F} - \mathbf{1}) = \frac{1}{2} (\mathbf{C} - \mathbf{1}) \quad (9)$$

The tensor $\mathbf{C} = \mathbf{F}^T \mathbf{F}$ is the right Cauchy-Green tensor. In component form the strain tensor \mathbf{E} can be written as $\mathbf{E} = E_{AB} \mathbf{E}_A \otimes \mathbf{E}_B$ with $E_{AB} = \frac{1}{2} (F_{iA} F_{iB} - \delta_{AB})$. The Kronecker symbol δ_{AB} denotes the components of the unit tensor $\mathbf{1}$. The Green-Lagrange strain measure describes arbitrary rigid body motions correctly. Often the Green-Lagrange strain tensor \mathbf{E} is expressed in terms of the displacement gradient. This yields with (8) $\mathbf{E} = \frac{1}{2} (\mathbf{H} + \mathbf{H}^T + \mathbf{H}^T \mathbf{H})$. The higher order term $\mathbf{H}^T \mathbf{H}$ depicts the nonlinear part of the Green-Lagrange strain tensor. Within the geometrically linear theory this term is neglected, hence \mathbf{E} reduces to the linear strain measure $\boldsymbol{\varepsilon}$

$$\boldsymbol{\varepsilon} = \frac{1}{2} (\mathbf{H} + \mathbf{H}^T) = \frac{1}{2} (u_{A,B} + u_{B,A}) \mathbf{E}_A \otimes \mathbf{E}_B. \quad (10)$$

The poplar decomposition of the deformation gradient splits the deformation gradient in a multiplicative way in a proper orthogonal rotation tensor \mathbf{R} (with $\mathbf{R}^{-1} = \mathbf{R}^T$) and the symmetrical stretch tensors \mathbf{U} , \mathbf{V} , see e.g. Ogden (1984)

$$\mathbf{F} = \mathbf{R} \mathbf{U} = \mathbf{V} \mathbf{R}. \quad (11)$$

Due to the orthogonality of \mathbf{R} one can write the right Cauchy-Green tensor in terms of \mathbf{U} : $\mathbf{C} = \mathbf{F}^T \mathbf{F} = \mathbf{U}^T \mathbf{R}^T \mathbf{R} \mathbf{U} = \mathbf{U}^T \mathbf{U} = \mathbf{U}^2$. The last result follows from the symmetry of \mathbf{U} . Since $\mathbf{C} = \mathbf{U}^2$ it can be easily shown that the spectral decomposition of the right Cauchy-Green tensor is given by

$$\mathbf{C} = \sum_{i=1}^3 \lambda_i^2 \mathbf{N}_i \otimes \mathbf{N}_i. \quad (12)$$

The stretch tensors can be computed via spectral decomposition

$$\mathbf{U} = \sum_{i=1}^3 \lambda_i \mathbf{N}_i \otimes \mathbf{N}_i \quad \mathbf{V} = \sum_{i=1}^3 \lambda_i \mathbf{n}_i \otimes \mathbf{n}_i \quad (13)$$

The principal values λ_i of the stretch tensors are called principal stretches. They are equal for \mathbf{U} and \mathbf{V} . The eigenvectors \mathbf{N}_i of \mathbf{U} are related to the reference configuration. The eigenvectors \mathbf{n}_i of \mathbf{V} are referred to the spatial configuration.

With respect to the spatial configuration $\varphi(B)$ the left Cauchy-Green tensor can be defined

$$\mathbf{b} = \mathbf{F} \mathbf{F}^T = \mathbf{V} \mathbf{R} \mathbf{R}^T \mathbf{V}^T = \mathbf{V}^2. \quad (14)$$

In case of incompressibility, that plays a prominent role in rubber materials and metal plasticity, the constraint condition $\det \mathbf{F} = J = 1$ holds. To account for this kinematic constraint the multiplicative decomposition of the deformation gradient

$$\mathbf{F} = J^{\frac{1}{3}} \widehat{\mathbf{F}} \quad \widehat{\mathbf{F}} = J^{-\frac{1}{3}} \mathbf{F} \quad (15)$$

was introduced in Flory (1961). It preserves a priori the volume of $\widehat{\mathbf{F}}$ (isochoric motion), since $\det \widehat{\mathbf{F}} \equiv 1$.

By inserting (15) in (9) one obtains a relation between the isochoric part of the right Cauchy-Green deformation tensor $\widehat{\mathbf{C}}$ and \mathbf{C}

$$\widehat{\mathbf{C}} = \widehat{\mathbf{F}}^T \widehat{\mathbf{F}} = J^{-\frac{2}{3}} \mathbf{F}^T \mathbf{F} = J^{-\frac{2}{3}} \mathbf{C}. \quad (16)$$

This multiplicative split corresponds to an additive decomposition of the strain tensor in the geometrically linear theory

$$\boldsymbol{\epsilon} = \mathbf{e}_D + \frac{1}{3} \operatorname{tr} \boldsymbol{\epsilon} \mathbf{1}. \quad (17)$$

1.2 Balance Equations

Differential equations that describe the local balance equations are introduced in this section. These are the balance of mass, balance of linear and angular momentum.

Balance of mass For processes in which the mass of the system is conserved the change one has ($\dot{m} = 0$). Hence an infinitesimal mass element in initial and current configuration has to be equal which leads to

$$\rho dv = \rho_0 dV. \quad (18)$$

Here ρ_0 and ρ are the densities in initial and current configuration, respectively. With Eq. (7) the volume elements dV and dv can be transformed leading to the Lagrangian description of the mass balance $\rho_0 = J \rho$.

Balance of linear and angular momentum The balance of linear momentum can be expressed in its local form by

$$\text{div } \boldsymbol{\sigma} + \rho \bar{\mathbf{b}} = \rho \dot{\mathbf{v}}, \quad \sigma_{ik,i} + \rho \bar{b}_k = \rho \dot{v}_k. \quad (19)$$

The stress tensor $\boldsymbol{\sigma}$ is called Cauchy stress tensor. $\rho \dot{\mathbf{v}}$ describes the inertial forces that can be neglected in case of purely static investigations. The stress vector \mathbf{t} can be obtained using the Cauchy's theorem

$$\mathbf{t} = \boldsymbol{\sigma} \mathbf{n}, \quad t_i = \sigma_{ik} n_k. \quad (20)$$

The angular momentum yields after some manipulations the local balance of angular momentum which simply demands the symmetry of the Cauchy stress tensor

$$\boldsymbol{\sigma} = \boldsymbol{\sigma}^T, \quad \sigma_{ik} = \sigma_{ki}. \quad (21)$$

Introduction of different stress tensors Equations (19) and (21) are referred to the current configuration. In finite element formulations it can be desirable to relate these equations to the initial configuration B . This leads with Nanson's formula (6) to

$$\int_{\partial\varphi(B)} \boldsymbol{\sigma} \mathbf{n} da = \int_{\partial B} \boldsymbol{\sigma} J \mathbf{F}^{-T} \mathbf{N} dA = \int_{\partial B} \mathbf{P} \mathbf{N} dA. \quad (22)$$

The relation defines the first Piola-Kirchhoff stress tensor \mathbf{P} that can be written in terms of the Cauchy stress

$$\mathbf{P} = J \boldsymbol{\sigma} \mathbf{F}^{-T} \quad P_{Ak} = J \sigma_{ik} (F_{iA})^{-1}. \quad (23)$$

\mathbf{P} is a two-field tensor with one basis referred to the current and the other to the initial configuration.

Often it is convenient to work totally in the initial configuration. For this purpose the second Piola-Kirchhoff stress tensor

$$\mathbf{S} = \mathbf{F}^{-1} \mathbf{P} = J \mathbf{F}^{-1} \boldsymbol{\sigma} \mathbf{F}^{-T}, \quad (24)$$

$$S_{AB} = (F_{Ai})^{-1} P_{Bi} = J (F_{Ai})^{-1} \sigma_{ik} (F_{kB})^{-1}. \quad (25)$$

was introduced. It is symmetric, but a pure mathematical quantity that generally cannot be interpreted as a physical measure for stress.

Besides the Cauchy stress tensor $\boldsymbol{\sigma}$ the Kirchhoff stress tensor

$$\boldsymbol{\tau} = \mathbf{F} \mathbf{S} \mathbf{F}^T, \quad \boldsymbol{\tau} = J \boldsymbol{\sigma}. \quad (26)$$

can be used. For some formulations the Biot stress tensor can be applied which is defined by

$$\mathbf{T}_B = \mathbf{R}^T \mathbf{P}. \quad (27)$$

Balance equations with respect to the initial configuration By using the first Piola-Kirchhoff stress tensor the local balance of linear momentum (19) can be recast in the initial configuration

$$\text{DIV } \mathbf{P} + \rho_0 \bar{\mathbf{b}} = \rho_0 \dot{\mathbf{v}} \quad (28)$$

where DIV denotes the divergence operation with respect to the coordinates of the initial configuration. The balance of angular momentum (21) yields with (23)

$$\mathbf{P} \mathbf{F}^T = \mathbf{F} \mathbf{P}^T. \quad (29)$$

This relation depicts that the first Piola-Kirchhoff stress tensor is nonsymmetric. The balance of angular momentum in terms of the second Piola-Kirchhoff stress tensor leads to $\mathbf{S} = \mathbf{S}^T$ which shows the symmetry of \mathbf{S} .

1.3 Constitutive Equations

For the solution of boundary or initial value problems in solid mechanics equations are needed that characterize the material response of a body. Here only isotropic elastic materials will be considered under the assumption of hyperelastic behavior, see e.g. Ogden (1984). This description is valid for materials that undergo finite deformations. In case of small strains these constitutive relations reduce to the classical law of Hooke.

The constitutive equation for the second Piola-Kirchhoff stress tensor can be derived from the potential ψ in case of a hyper elastic material. ψ describes the strain energy stored in the body. The derivative of ψ with respect to the right Cauchy-Green tensor yields

$$\mathbf{S} = 2 \rho_0 \frac{\partial \psi(\mathbf{C})}{\partial \mathbf{C}}; \quad S_{AB} = 2 \rho_0 \frac{\partial \psi(C_{CD})}{\partial C_{AB}}. \quad (30)$$

For isotropic material behavior a strain energy function can be introduced that only depends on the invariants of the strain tensors

$$\psi(\mathbf{C}) = \psi(I_C, II_C, III_C). \quad (31)$$

The invariants I_C , II_C , III_C are defined in the standard way:

$$I_C = \text{tr} \mathbf{C}, \quad II_C = \frac{1}{2} [(\text{tr} \mathbf{C})^2 - \text{tr}(\mathbf{C}^2)] \quad \text{and} \quad III_C = \det \mathbf{C}.$$

With the relations

$$\begin{aligned} I_C &= \lambda_1^2 + \lambda_2^2 + \lambda_3^2 \\ II_C &= \lambda_1^2 \lambda_2^2 + \lambda_2^2 \lambda_3^2 + \lambda_3^2 \lambda_1^2 \\ III_C &= \lambda_1^2 \lambda_2^2 \lambda_3^2 \end{aligned} \quad (32)$$

one can express the invariants in terms of the principal stretches λ_i^2 of \mathbf{C} . Then the strain energy function assumes the form

$$\psi(\mathbf{C}) = \psi(\lambda_1^2, \lambda_2^2, \lambda_3^2). \quad (33)$$

The isotropic constitutive Eq. (30) can also be expressed in quantities related to the current configuration. With Eq. (25) one obtains for the Cauchy stress $\boldsymbol{\sigma} = J^{-1} \mathbf{F} \mathbf{S} \mathbf{F}^T$ and hence by considering (18)

$$\boldsymbol{\sigma} = 2 \rho \mathbf{F} \frac{\partial \psi(\mathbf{C})}{\partial \mathbf{C}} \mathbf{F}^T.$$

It can be shown that this equation is equivalent to

$$\boldsymbol{\sigma} = 2 \rho \mathbf{b} \frac{\partial \psi(\mathbf{b})}{\partial \mathbf{b}}. \quad (34)$$

Constitutive equations of the form (31) are still very complex because ψ can be an arbitrary function of the invariants. It is desirable to formulate material functions in nonlinear elasticity with a minimum number of constitutive parameters. To shorten notation $W = \rho_0 \psi$ is introduced in the following to define the strain energy function. The choice of

$$W(I_C) = g(J) + \frac{1}{2} \mu (I_C - 3) \quad \text{with} \quad J = \sqrt{\det \mathbf{C}} \quad (35)$$

yields the special case of a compressible Neo-Hooke material. A special ansatz can be selected for $g(J)$ in (35)

$$g(J) = c (J^2 - 1) - d \ln J - \mu \ln J \quad \text{with} \quad c > 0, d > 0. \quad (36)$$

The constitutive parameters Λ, μ are known as the Lamé constants.

Other strain energy functions for incompressible rubber materials are the so called Mooney–Rivlin materials

$$W(I_C, II_C) = c_1 (I_C - 3) + c_2 (II_C - 3). \quad (37)$$

For a complete formulation of an incompressible problem the incompressibility constraint ($J = 1$) has to be considered.

In case of geometrically linear materials a linear relation between the stresses and the linear strains is proposed. This is given by

$$\boldsymbol{\sigma} = \Lambda \operatorname{tr} \boldsymbol{\epsilon} \mathbf{1} + 2\mu \boldsymbol{\epsilon} \quad (38)$$

in terms of the two Lamé constants Λ and μ . Since in the linear case we do not have to distinguish different stress measures, we use here for convenience the Cauchy stress.

In finite elasticity of rubber materials one splits of the deformation in a volumetric part represented by J and the isochoric part described by $\widehat{\mathbf{C}}$, see (16), since both part can depict different material behavior. This split is useful in mixed finite element formulations when quasi-incompressible materials are described by special numerical formulations since the split permits a different treatment of the incompressible part. One possibility for the formulation of the constitutive equation is given by an additive split of the strain energy function in its volumetric and isochoric parts: $W(\widehat{\mathbf{C}}, J) = \widehat{W}(\widehat{\mathbf{C}}) + U(J)$. This leads for a strain energy function that is analogous to the one introduced in (35)

$$W(\widehat{\mathbf{C}}, J) = U(J) + \frac{1}{2} \mu (I_{\widehat{\mathbf{C}}} - 3). \quad (39)$$

Here the term $U(J)$ is different from $g(J)$: $U(J) = \frac{K}{4} (J^2 - 1) - \frac{K}{2} \ln J$ where K denotes the modulus of compression.²

For the special choice of the strain energy function (39) one specifies

$$\mathbf{S}_{ISO} = \mu J^{-\frac{2}{3}} \left(\mathbf{1} - \frac{1}{3} \operatorname{tr} \mathbf{C} \mathbf{C}^{-1} \right), \quad \mathbf{S}_{VOL} = \frac{K}{2} (J^2 - 1) \mathbf{C}^{-1}. \quad (40)$$

The transformation to the current configuration yields for the Kirchhoff stress tensor introduced in (27) together with the operator $\operatorname{dev}(\bullet) = (\bullet) - \frac{1}{3} \operatorname{tr}(\bullet) \mathbf{1}$ for (40)

$$\boldsymbol{\tau} = J p \mathbf{1} + \operatorname{dev} \widehat{\boldsymbol{\tau}} = \tau_{vol} \mathbf{1} + \boldsymbol{\tau}_{iso}. \quad (41)$$

²Note that this split represents physically a different strain energy function than (35).

This depicts the split of the stress tensor into a volumetric and an isochoric part clearly. The following definitions were used in (41)

$$p = \frac{\partial U}{\partial J} \quad \text{and} \quad \hat{\boldsymbol{\tau}} = \hat{\mathbf{F}}^2 \frac{\partial \hat{W}}{\partial \hat{\mathbf{C}}} \hat{\mathbf{F}}^T. \quad (42)$$

In case of small strains, we can use (17) to represent the linear elastic constitutive equation by

$$\boldsymbol{\sigma} = \Lambda \operatorname{tr} \boldsymbol{\epsilon} \mathbf{1} + 2\mu \left(\mathbf{e}_D + \frac{1}{3} \operatorname{tr} \boldsymbol{\epsilon} \right). \quad (43)$$

This equation can be rewritten with the modulus of compression $K = \Lambda + \frac{2}{3}\mu$ as

$$\boldsymbol{\sigma} = K \operatorname{tr} \boldsymbol{\epsilon} \mathbf{1} + 2\mu \mathbf{e}_D. \quad (44)$$

With the introduction of the pressure

$$p = K \operatorname{tr} \boldsymbol{\epsilon} \quad (45)$$

and the deviatoric stress

$$\mathbf{s} = 2\mu \mathbf{e}_D \quad (46)$$

the stress can be decomposed in a deviatoric and volumetric part

$$\boldsymbol{\sigma} = p \mathbf{1} + \mathbf{s}. \quad (47)$$

1.4 Weak Forms of Balance of Momentum

The principle of virtual work is an equivalent formulation of the balance of linear and angular momentum (19) or (28). In the mathematical literature it is called weak form of the partial differential equation. Since no further assumptions, like existence of a potential, are made, the weak form is applicable to general problems like inelastic materials, friction, etc. The derivation of the weak form starts from the equation of linear momentum ($\operatorname{Div} \mathbf{P} + \rho_0 \bar{\mathbf{b}} = \rho_0 \dot{\mathbf{v}}$) which is multiplied scalar by a vector valued function $\boldsymbol{\eta} = \{\boldsymbol{\eta} \mid \boldsymbol{\eta} = \mathbf{0} \text{ auf } \partial B_u\}$ —often called virtual displacement or test function. The following integration over the volume of the solid yields, together with a partial integration of the first term, application of the divergence theorem and introduction of the traction boundary condition the weak form of linear momentum

$$\int_B \mathbf{P} \cdot \operatorname{Grad} \boldsymbol{\eta} dV - \int_B \rho_0 (\bar{\mathbf{b}} - \dot{\mathbf{v}}) \cdot \boldsymbol{\eta} dV - \int_{\partial B_\sigma} \bar{\mathbf{t}} \cdot \boldsymbol{\eta} dA = 0. \quad (48)$$

The gradient of the test function η can also be interpreted as variation $\delta \mathbf{F}$ of the deformation gradient. In the weak form (48) the first Piola-Kirchhoff stress tensor can be replaced by the second Piola-Kirchhoff stress tensor leading to

$$\mathbf{P} \cdot \text{Grad } \eta = \mathbf{S} \cdot \mathbf{F}^T \text{Grad } \eta = \mathbf{S} \cdot \frac{1}{2} (\mathbf{F}^T \text{Grad } \eta + \text{Grad}^T \eta \mathbf{F}) = \mathbf{S} \cdot \delta \mathbf{E}, \quad (49)$$

where the fact has been used that the scalar product of a symmetrical tensor (here \mathbf{S}) with a antisymmetrical part of a tensor is zero. $\delta \mathbf{E}$ denotes the variation of the Green-Lagrange strain tensor. Using (49) equation (48) can be rewritten as

$$\int_B \mathbf{S} \cdot \delta \mathbf{E} dV - \int_B \rho_0 (\bar{\mathbf{b}} - \dot{\mathbf{v}}) \cdot \eta dV - \int_{\partial B_\sigma} \bar{\mathbf{t}} \cdot \eta dA = 0. \quad (50)$$

The first term in (50) denotes the internal virtual work also called stress divergence term. The last two terms describe the virtual work of the applied loading and the inertia term.

The transformation of the weak form (48) to the current or spatial configuration is performed by using the transformation of the first Piola-Kirchhoff stress tensor to the Cauchy stress tensor, see (23): $\boldsymbol{\sigma} = \frac{1}{J} \mathbf{P} \mathbf{F}^T$. This leads to

$$\mathbf{P} \cdot \text{Grad } \eta = J \boldsymbol{\sigma} \mathbf{F}^{-T} \cdot \text{Grad } \eta = J \boldsymbol{\sigma} \cdot \text{Grad } \eta \mathbf{F}^{-1} = J \boldsymbol{\sigma} \cdot \text{Grad } \eta.$$

Furthermore we have with (7) $dv = J dV$ which is equivalent to $\rho = \rho_0 J$. With these relations the weak form (48) can be written in terms of the current configuration

$$\int_{\varphi(B)} \boldsymbol{\sigma} \cdot \text{Grad } \eta dv - \int_{\varphi(B)} \rho (\bar{\mathbf{b}} - \dot{\mathbf{v}}) \cdot \eta dv - \int_{\varphi(\partial B_\sigma)} \hat{\mathbf{t}} \cdot \eta da = 0. \quad (51)$$

The symmetry of the Cauchy stress tensor facilitates the replacement of the spatial gradient by its symmetric part. Hence with the definition

$$\nabla^S \eta = \frac{1}{2} (\text{Grad } \eta + \text{Grad}^T \eta) \quad (52)$$

the weak form with respect to the spatial configuration follows

$$\int_{\varphi(B)} \boldsymbol{\sigma} \cdot \nabla^S \eta dv - \int_{\varphi(B)} \rho (\bar{\mathbf{b}} - \dot{\mathbf{v}}) \cdot \eta dv - \int_{\varphi(\partial B_\sigma)} \hat{\mathbf{t}} \cdot \eta da = 0. \quad (53)$$

For the geometrical linear theory the weak form is formally equivalent to (53). Only the operator defined in (52) has to be evaluated with respect to the coordinates of the initial configuration as well as the integrals

$$g^{lin}(\mathbf{u}, \boldsymbol{\eta}) = \int_B \boldsymbol{\sigma} \cdot \nabla_X^S \boldsymbol{\eta} dv - \int_B \rho \bar{\mathbf{b}} \cdot \boldsymbol{\eta} dv - \int_{\partial B_\sigma} \hat{\mathbf{t}} \cdot \boldsymbol{\eta} da = 0 \quad (54)$$

with $\nabla_X^S \boldsymbol{\eta} = \frac{1}{2} (\text{Grad } \boldsymbol{\eta} + \text{Grad}^T \boldsymbol{\eta})$.

1.5 Variational Functionals

In this section two variational functionals will be discussed which can alternatively be applied within the discretization process of the finite element method.

Based on this strain energy W the classical principle of minimum of potential energy can be formulated for the finite deformation theory.³ Here one has in general consider that deformations can occur which are unstable. Due to that only a stationary value of the potential can be reached. We assume further that the applied loads are conservative which means path independent. Then one can state for static problems

$$\Pi(\boldsymbol{\varphi}) = \int_B [W(\mathbf{C}) - \rho_0 \bar{\mathbf{b}} \cdot \boldsymbol{\varphi}] dV - \int_{\partial B_\sigma} \bar{\mathbf{t}} \cdot \boldsymbol{\varphi} dA \implies \text{STAT}. \quad (55)$$

Of all possible deformations $\boldsymbol{\varphi}$ the ones which make Π stationary fulfill the equilibrium equation. The stationary value of (55) can be computed by the variation of Π with respect to the deformation. This is achieved by the directional derivative

$$\delta \Pi = D \Pi(\boldsymbol{\varphi}) \cdot \boldsymbol{\eta} = \left. \frac{d}{d\alpha} \Pi(\boldsymbol{\varphi} + \alpha \boldsymbol{\eta}) \right|_{\alpha=0}, \quad (56)$$

which is also called first variation of Π . The associated mathematical operation yields

$$D \Pi(\boldsymbol{\varphi}) \cdot \boldsymbol{\eta} = \int_B \left[\frac{\partial W}{\partial \mathbf{C}} \cdot D \mathbf{C} \cdot \boldsymbol{\eta} - \rho_0 \bar{\mathbf{b}} \cdot \boldsymbol{\eta} \right] dV - \int_{\partial B_\sigma} \bar{\mathbf{t}} \cdot \boldsymbol{\eta} dA = G(\mathbf{u}, \boldsymbol{\eta}) = 0. \quad (57)$$

The directional derivative of the right Cauchy-Green strain tensor can be written in terms of the Green-Lagrange strain tensor: $D \mathbf{C} \cdot \boldsymbol{\eta} = 2 D \mathbf{E} \cdot \boldsymbol{\eta}$.⁴

³The construction of such principle has advantages. One of them is that the development of efficient algorithms for the solution of the nonlinear equations can be based on optimization strategies.

⁴This result corresponds to the variation $\delta \mathbf{E}$, defined already (49). The partial derivative of W with respect to \mathbf{C} leads to the second Piola-Kirchhoff stress tensor \mathbf{S} , see (30): $\mathbf{S} = 2 \partial W / \partial \mathbf{C}$. Hence Eq. (57) is equivalent to the weak form (50) for a hyperelastic material.

The stationary value of (55) can also be computed by the variation of Π with respect to the deformation. For this purpose the directional derivative (56) is applied. The application of this mathematical operation yields

$$D\Pi(\varphi) \cdot \boldsymbol{\eta} = \int_B \left[\frac{\partial W}{\partial \boldsymbol{\varphi}} \cdot \boldsymbol{\eta} - \rho_0 \bar{\mathbf{b}} \cdot \boldsymbol{\eta} \right] dV - \int_{\partial B_\sigma} \bar{\mathbf{t}} \cdot \boldsymbol{\eta} dA = 0. \quad (58)$$

Note that weak form (58) is obtained directly by the variation of (55). Hence equation (58) is equivalent to the weak form (57) for hyperelastic materials.

Another more general variational principle is the Hu–Washizu principle, see Washizu (1975). It has gained significance during the last years for the construction of finite elements. This principles can be derived by writing the weak formulation with additional constraints that contain kinematics and constitutive equations. Hence deformations, strains and stresses occur as independent variables. Once this principle is constructed its variation with respect to all variables yields the static equilibrium equations, the kinematical relations and the constitutive equation. The nonlinear version of the Hu–Washizu principle can formulated by using any set of work conjugated variables. Here, we will state it in terms of the deformation gradient \mathbf{F} , the first Piola-Kirchhoff stress tensor \mathbf{P} and the Deformation φ

$$\begin{aligned} \Pi(\varphi, \mathbf{F}, \mathbf{P}) = & \int_B [W(\mathbf{F}) + \mathbf{P} \cdot (\text{Grad } \varphi - \mathbf{F})] dV \\ & - \int_B \varphi \cdot \rho_0 \bar{\mathbf{b}} dV - \int_{\partial B_\sigma} \varphi \cdot \hat{\mathbf{t}} dA. \end{aligned} \quad (59)$$

The variation, according to the definition of the directional derivative given above, yields now three independent equations

$$\begin{aligned} D\Pi(\varphi, \mathbf{F}, \mathbf{P}) \cdot \boldsymbol{\eta} = & \int_B (\mathbf{P} \cdot \text{Grad } \boldsymbol{\eta} - \boldsymbol{\eta} \cdot \rho_0 \bar{\mathbf{b}}) dV - \int_{\partial B_\sigma} \boldsymbol{\eta} \cdot \hat{\mathbf{t}} dA = 0, \\ D\Pi(\varphi, \mathbf{F}, \mathbf{P}) \cdot \mathbf{Q} = & \int_B \mathbf{Q} \cdot (\text{Grad } \varphi - \mathbf{F}) dV = 0, \\ D\Pi(\varphi, \mathbf{F}, \mathbf{P}) \cdot \mathbf{A} = & \int_B \mathbf{A} \cdot \left(\frac{\partial W}{\partial \mathbf{F}} - \mathbf{P} \right) dV = 0 \end{aligned} \quad (60)$$

where $\boldsymbol{\eta}$, \mathbf{Q} and \mathbf{A} are the virtual displacements, the virtual stresses and the virtual strains, respectively. Observe that they represent the weak form (48), the kinematical relation (4) and a hyperelastic constitutive equation for \mathbf{P} . Note further that the last two terms can be interpreted as constraint terms which have to be fulfilled additionally together with the linear momentum equation. In that case \mathbf{Q} and \mathbf{A} are Lagrangian multipliers.

The Hu–Washizu principle was originally derived in Washizu (1975) for small elastic deformations. It then is stated in terms of the strain tensor ϵ , the first stress tensor σ and the displacement \mathbf{u}

$$\begin{aligned} \Pi(\mathbf{u}, \epsilon, \sigma) = & \int_B \left[\frac{\Lambda}{2} (\text{tr} \epsilon)^2 + \mu \epsilon \cdot \epsilon + \sigma \cdot (\nabla_X^S \mathbf{u} - \epsilon) \right] dV \\ & - \int_B \varphi \cdot \rho_0 \bar{\mathbf{b}} dV - \int_{\partial B_\sigma} \varphi \cdot \hat{\mathbf{t}} dA. \end{aligned} \quad (61)$$

The variation, according to the definition of the directional derivative given above, yields again three independent equations.

A special form of the Hu–Washizu variational principle can be applied for the construction of finite elements which have to represent nearly incompressible material behavior. Since incompressibility is associated with a constraint for the volumetric deformation ($J \equiv 1$), one can use the split (15) to distinguish volumetric and isochoric parts of the deformation. Based on this idea Simo et al. (1985) formulated a three-field functional which is only defined for the volumetric part of the deformation. Hence the independent variable are now the deformation φ , the pressure p and a strain variable θ which is equivalent to J . The last variable has to fulfill the constraint condition $\theta = J$. With the multiplicative split of the deformation gradient one obtains the split into volumetric and deviatoric parts. Note that we have in relation (15) $\hat{\mathbf{F}} = J^{-\frac{1}{3}} \text{Grad } \varphi$. Furthermore $\bar{\mathbf{C}} = \theta^{\frac{2}{3}} J^{-\frac{2}{3}} \mathbf{C} = \theta^{\frac{2}{3}} \hat{\mathbf{C}}$ holds with (16). Also the strain energy function has to be defined on the basis of the new variables: $W(\theta^{\frac{2}{3}} \hat{\mathbf{C}})$. Using the additive split $W = W(\theta) + W(\hat{\mathbf{C}})$, see (39), the following three-field variational functional can be defined

$$\begin{aligned} \Pi(\varphi, p, \theta) = & \int_B [W(\hat{\mathbf{C}}) + W(\theta) + p(J - \theta)] dV \\ & - \int_B \varphi \cdot \rho_0 \bar{\mathbf{b}} dV - \int_{\partial B_\sigma} \varphi \cdot \hat{\mathbf{t}} dA. \end{aligned} \quad (62)$$

This form is actually a mixture of a Hu–Washizu principle for the pressure p and the volumetric deformation J and a deformation based functional like (55) for $\hat{\mathbf{C}}$.

The Hu–Washizu principle is the most general principle which depends on three independent fields. Based on the fulfillment of a constraints we can eliminate such constraints directly. This yields two-field formulation with displacements and stresses as primary variables. The adequate Hellinger–Reissner functional can be written for small strains as

$$\Pi_{HR}(\sigma, \mathbf{u}) = \int_B \sigma \cdot \nabla_X^S \mathbf{u} dV - \frac{1}{2} \int_B \sigma \cdot \mathcal{C}^{-1}[\sigma] dV - \int_B \hat{\mathbf{b}} \cdot \mathbf{u} dV - \int_{\partial B_\sigma} \hat{\mathbf{t}} \cdot \mathbf{u} dA. \quad (63)$$

Here \mathcal{C} is the constitutive tensor which relates strains and stresses in case of linear elasticity, see (38),

$$\boldsymbol{\sigma} = \mathcal{C} [\boldsymbol{\epsilon}(\mathbf{u})] = \mathcal{C} [\nabla_X^S \mathbf{u}]. \quad (64)$$

$\hat{\mathbf{b}}$ and $\hat{\mathbf{t}}$ are the applied body forces and boundary tractions, respectively.

The variation of this variational functional yields

$$\begin{aligned} D\Pi \cdot \boldsymbol{\eta} &= \int_B \boldsymbol{\sigma} \cdot \nabla_X^S \boldsymbol{\eta} dV - \int_B \hat{\mathbf{b}} \cdot \boldsymbol{\eta} dV - \int_{\partial B_\sigma} \hat{\mathbf{t}} \cdot \boldsymbol{\eta} dA = 0, \\ D\Pi \cdot \boldsymbol{\tau} &= \int_B \boldsymbol{\tau} \cdot \nabla_X^S \mathbf{u} dV - \int_B \boldsymbol{\tau} \cdot \mathcal{C}^{-1} [\boldsymbol{\sigma}] dA = 0. \end{aligned} \quad (65)$$

The first equation represents the weak form of equilibrium. The second equation is the weak statement of the constitutive equation. Hence the two-field Hellinger–Reissner principle has besides the weak form of equilibrium one additional constraint equation, which is the inverse of constitutive Eq. (64).

More general, we have the relation stemming from the Legendre transformation

$$W(\boldsymbol{\epsilon}) = \boldsymbol{\sigma} \cdot \boldsymbol{\epsilon} - U(\boldsymbol{\sigma}) \quad (66)$$

in linear elasticity we have $W(\boldsymbol{\epsilon}) = \frac{1}{2} \boldsymbol{\epsilon} \cdot \mathcal{C} [\boldsymbol{\epsilon}]$ which yields with (64)

$$U(\boldsymbol{\sigma}) = \frac{1}{2} \boldsymbol{\sigma} \cdot \mathcal{C}^{-1} [\boldsymbol{\sigma}]. \quad (67)$$

Hence it is easy to see that the first two terms in (63) are equivalent to the integral of the strain energy $W(\boldsymbol{\epsilon})$.

Another version of a functional has as only unknowns the stresses. This is based on the dual formulation

$$U(\boldsymbol{\sigma}) = \frac{1}{2} \int_B \boldsymbol{\sigma} \cdot \mathcal{C}^{-1} [\boldsymbol{\sigma}] dV \quad (68)$$

in which the complementary energy $U(\boldsymbol{\sigma})$ has to be minimized by a stress field which fulfills the strong form of linear and angular momentum (19) and (21) in B for the case of statics and the stress boundary conditions (Neumann boundary conditions) on ∂B_σ . It is of course complicated to find a stress field which fulfills these local conditions. Hence one can add the linear momentum to (68) by using the Lagrangian multiplier method

$$\frac{1}{2} \int_B \boldsymbol{\sigma} \cdot \mathcal{C}^{-1} [\boldsymbol{\sigma}] dV + \int_B (\operatorname{div} \boldsymbol{\sigma} + \rho \mathbf{b}) \cdot \mathbf{u} dV \rightarrow \text{EXTR}. \quad (69)$$

Now the stresses have to be computed for fields which fulfill the divergence operator and the angular momentum (21) in B and the Neumann boundary conditions on ∂B_σ . The Lagrange multiplier \mathbf{u} can be interpreted as a displacement. Since it is not simple to find stable finite element discretizations for (69), see Brezzi and Fortin (1991), one can relax the strong symmetry condition (21) of the stress field, see e.g. Fraeijs de Veubeke (1975), Arnold et al. (1984) and Stenberg (1988). This yields the modified functional

$$\frac{1}{2} \int_B \boldsymbol{\sigma} \cdot \mathbb{C}^{-1} [\boldsymbol{\sigma}] dV + \int_B (\operatorname{div} \boldsymbol{\sigma} + \rho \mathbf{b}) \cdot \mathbf{u} dV + \int_B \boldsymbol{\sigma} \cdot \boldsymbol{\beta} dV \rightarrow EXTR. \quad (70)$$

Here the stress field has to fulfill the divergence operator and the Neumann boundary conditions. The additional Lagrange multiplier $\boldsymbol{\gamma}$ is associated with the linear rotation field. At the extremum it has the value $\boldsymbol{\beta} = \frac{1}{2} (\nabla \mathbf{u} - \nabla^T \mathbf{u})$. Variation of (70) leads to the weak form for the three independent fields $\boldsymbol{\sigma}$, \mathbf{u} and $\boldsymbol{\beta}$

$$\begin{aligned} \int_B \boldsymbol{\tau} \cdot \mathbb{C}^{-1} [\boldsymbol{\sigma}] dV + \int_B \operatorname{div} \boldsymbol{\tau} \cdot \mathbf{u} + \int_B \boldsymbol{\tau} \cdot \boldsymbol{\beta} dV &= 0, \\ \int_B (\operatorname{div} \boldsymbol{\sigma} + \rho \mathbf{b}) \cdot \boldsymbol{\eta} dV &= 0, \\ \int_B \boldsymbol{\sigma} \cdot \boldsymbol{\gamma} dV &= 0. \end{aligned} \quad (71)$$

Here $\boldsymbol{\tau}$, $\boldsymbol{\eta}$ and $\boldsymbol{\gamma}$ are the test functions.

1.6 Linearization of Variational Formulations

The solutions of nonlinear initial or boundary value problems in solid mechanics can be obtained in general only by employing approximate solution techniques. Since many of these methods—like also the finite element method—rely on a variational formulation of the field equations, the basis for numerical methods are provided by the weak forms of the associated field equations.

For the solution of the set of nonlinear equations many different algorithms are known. Often Newton's method is applied since it possesses the advantage of a quadratic convergence close to the solution point. In case of Newton's method, an improved solution is obtained from the Taylor series expansion of the nonlinear equation at the already computed approximate solution. This Taylor expansion corresponds in finite element applications to the linearization of the weak form, or in solid mechanics to the linearization of the virtual work or variational principles and can be obtained by the directional derivative.

In this contribution, the automatic tool *AceGen* is employed to generate the finite element formulations. This tool which is based on *Mathematica* has the ability to automatically derive the linearizations of weak form expressions, thus there is no need to derive explicit expressions for the linearization of the weak forms used within the finite element method.

2 Finite Element Methods

Many formulation exists for the construction of finite elements. They are based on different interpolations and ansatz functions and different mathematical models related to the weak forms. The element formulations can be basically classified as follows.

- Finite elements with ansatz functions for the primary variables, in solid mechanics these are the deformations. Classically, the interpolation is provided by polynomials,
- Formulations based on mixed ansatz functions for different variables, like deformations, stresses, strains. Here polynomials of different order are applied to interpolate the field variables.
- Elements using Bezier interpolations, like isogeometric ansatz functions, in primal or mixed form.

In this contribution, we will discuss elements related to the first two points, for the third point see, e.g., Cottrell et al. (2009).

2.1 Requirements for Solid Elements

The ideal case for application of the finite method would be that one interpolation scheme could be used for a large class of problems. Due to several reasons that are discussed below, this is not possible. However, the search for such an element family has led to numerous scientific contributions in this area, for overviews, see, e.g., Zienkiewicz and Taylor (2000) and Wriggers (2008). The basic problem classes that arise in solid mechanics problems undergoing finite deformations are

- elastic deformations,
- inelastic deformations,
- deformations with volume constraints, like incompressibility or anisotropic uni-directional constraints,
- deformations, constraint by contact and interface conditions and
- deformations of thin solids, like beams, plates, and shells.

For these problem classes one would like to have elements that can predict deformation and stress fields in an accurate and efficient manner. Furthermore, the formula-

tions should be robust in the sense that they converge with respect to the necessary equilibrium iterations when applied in the large deformation range.

Based on these demands specific targets for the element development can be specified. Some of them are listed below.

- No sensitivity against mesh distortions, means that the element, undergoing large strain states, might deform very much and thus can change its shape. Thus, an element with convex geometry can become nonconvex. These types of distortions should not affect the overall solution behavior. But also mesh generation tools can create element geometries that are severely distorted.
- Good coarse mesh accuracy is needed when available computer resources are limited. In such cases, especially in three-dimensional applications the element should provide results with sufficient accuracy even for relative coarse meshes. This demand is in line with efficiency of the element formulation which means that computing effort at local element level should be as low as possible. Here, a small number of integrations points, no solution of extra equation systems provide efficient elements. An example for such element formulation can be found, e.g. in Reese (2005).
- Finite elements should be formulated such that the implementation of nonlinear constitutive equations is relatively simple. In that way, an interface can be created that allows even nonspecialists to apply a certain finite element to another class of constitutive equations.
- When constraint equations have to be considered within the finite element formulation, standard approaches with low-order interpolation tend to lock. This occurs for incompressible and anisotropic materials, but also certain elasto-plastic material equations and for thin, elements that undergo bending deformations for which standard interpolations lock, see e.g. Zienkiewicz and Taylor (1989) oder Hughes (1987) and Braess (1992).

Element ansatz functions that interpolate the deformation or displacement field within an element with first-order shape functions (bi- or tri-linear interpolation) do not converge properly when applied to bending problems and to problems where incompressible material is present. In the past different variational formulations have been explored in order to construct finite elements that can be used for this problem class. Some approaches are listed below.

- Reduced integration and stabilization is the most simple method to overcome locking behavior, see, e.g., Zienkiewicz et al. (1971). Many variants were discussed in the literature. It was shown the reduced integration on works together with stabilization, see e.g. Belytschko et al. (1984) and Reese and Wriggers (2000). These elements are in general *locking* free for incompressible deformations. They are not sensitive against mesh distortion and can be used for arbitrary constitutive equations. Due to the reduced integration these elements are very efficient (e.g., for an eight-node brick element only one Gauss point is needed). On the down side, the reduced integrated and stabilized elements rely often on artificial stabilization parameters. Hence, there exists cases, like some bending problems where the finite element solution depends on the stabilization parameter.

- Finite elements based on the mixed variational principle of Hu–Washizu type were successfully developed by Simo and co-workers who introduced the *enhanced strain* elements first for the geometrical linear theory, Simo and Rifai (1990) and then for large deformations, Simo and Armero (1992) and Simo et al. (1993)

2.2 Nonlinear Finite Element Formulations

In this contribution the tool *AceGen*, see Korelc (2011), is used to produce efficient finite element code with a minimum of effort. This package is a toolbox that is based on Mathematica (2011). It has the following advantages for developers of finite elements:

- automatic generation of finite element source code for different code environments, see Korelc (2002),
- short generation times, see Korelc (1997),
- produces residual vectors and tangent matrices automatically for complex applications,
- all relevant equations can be checked in debug mode.

The workflow when using *AceGen* can be basically described as follows

- initialize *AceGen*,
- initialize a template (type of finite element, e.g., a six-node triangle or a hexahedral element with eight nodes). This template defines automatically all essential variables related to such element, like number of nodes, etc.
- define the problem (mechanical, thermal,...):
 - define variables,
 - define shape functions and symbolically compute derivatives with respect to the selected coordinate systems,
 - compute symbolically kinematical variables and stresses (if needed, like, e.g., in the weak form),
 - define strain energy function or weak form,
- derive residual vector and tangent matrix symbolically,
- generate code and export code for the selected environment.

2.3 Three-Dimensional Finite Strain Element

To show the general procedure that has to be followed in order to derive finite elements, three-dimensional finite elements for finite strains are developed for a Neo-Hooke material based on the strain energy (55) and on the weak form (50).

Formulation based on the strain energy function In this approach, the finite element is developed based on the strain energy function with respect to the initial configuration. The strain energy can be written for a hyperelastic Neo-Hooke material as

$$W(\mathbf{u}) = \int_V \left\{ \frac{\lambda}{2} (J(\mathbf{u}) - 1)^2 + \frac{\mu}{2} [\text{tr} \mathbf{C}(\mathbf{u}) - 3 - 2 \log J(\mathbf{u})] \right\} dV. \quad (72)$$

with the Lamé constants λ and μ , the right Cauchy-Green tensor \mathbf{C} , see (9), and the Jacobian $J = \det \mathbf{F}$, see (8). All kinematic variables depend on the displacement field \mathbf{u} .

A finite element formulation will now be developed for the hexahedral element with tri-linear shape functions based on the isoparametric concept. In this formulation, the displacement field and the coordinated within the element are approximated by the same ansatz

$$\mathbf{u}_e = \sum_{I=1}^8 N_I(\xi, \eta, \zeta) \mathbf{u}_I \quad \mathbf{X}_e = \sum_{I=1}^8 N_I(\xi, \eta, \zeta) \mathbf{X}_I. \quad (73)$$

For the 8 noded brick element the shape functions N_I can be expressed as follows

$$N_I(\xi, \eta, \zeta) = \frac{1}{8} (1 + \xi_I \xi) (1 + \eta_I \eta) (1 + \zeta_I \zeta), \quad I = 1, \dots, 8 \quad (74)$$

where ξ_I , η_I and ζ_I are the nodal points in the reference element of the isoparametric formulation, for details see, e.g., Wriggers (2008).

Note that differentiation within the isoparametric formulation with respect to the physical coordinates \mathbf{X} has to be done by using the chain rule. By defining $\Xi = \{\xi, \eta, \zeta\}$ the differentiation of the displacement field with respect to \mathbf{X} , leading to the displacement gradient \mathbf{H} , see (8), can be written within the element e as

$$\mathbf{H}_e = \text{Grad } \mathbf{u} = \frac{\partial \mathbf{u}}{\partial \mathbf{X}} = \frac{\partial \mathbf{u}}{\partial \Xi} \frac{\partial \Xi}{\partial \mathbf{X}} = \mathbf{J}_e^{-T} \frac{\partial \mathbf{u}}{\partial \Xi} \quad (75)$$

where $\mathbf{J}_e = \frac{\partial \mathbf{X}}{\partial \Xi}$ is the Jacobi matrix of the transformation from the coordinates Ξ reference element to the actual physical coordinates \mathbf{X} of element e . After that the deformation gradient \mathbf{F} , its determinant J and the right Cauchy-Green tensor \mathbf{C} follow directly for the element e

$$\mathbf{F}_e = \mathbf{1} + \mathbf{H}_e, \quad J_e = \det \mathbf{F}_e \quad \text{and} \quad \mathbf{C}_e = \mathbf{F}_e^T \mathbf{F}_e. \quad (76)$$

Now all basic variable needed in (72) are defined and *AceGen* can be applied to derive the nonlinear hexahedral element. Here the basic steps are shown. For details regarding the use of this tool, see Korelc (2011).

Fig. 1 Initiation of *AceGen*

```
<<AceGen`;
SMSInitialize["H1element", "Environment" -> "AceFEM"];
```

Fig. 2 Basic template of the element

```
SMSTemplate[
  "SMSTopology" -> "H1"
  , "SMSDomainDataNames" ->
    { "E -elastic modulus", "ν -poisson ratio", ... }
  , "SMSDefaultData" -> { 21000, 0.3, ... }
  , "SMSSymmetricTangent" -> True
];
nen=SMSNoNodes; ndim=SMSNoDimensions;
np=SMSNoDOFGlobal;
```

The toolbox has to be started, see first line in Fig. 1. The second line defines the name of the generated element “H1element” and the finite element environment for which the element will be generated, in this case the program *AceFEM* associated with *AceGen*. However also elements can be generated for the commercial program ABAQUS and the research code FEAP, see Taylor (2011).

Next comes the selection of the template, here “H1” is related to the eight-noded hexahedral element, see Fig. 2. With this *AceGen* knows the dimension, the number of nodes and the number of unknowns. Furthermore input data related to the material model, loading,... are provided in this template.

In Fig. 3 the first line retrieves the material data in form of the Young’s modulus E and the Poisson ratio ν which are converted by an inbuilt function to the Lamé constants λ and μ in the next line. In the third and forth line the nodal values of the coordinates, \mathbf{X}_i and the displacements, \mathbf{u}_i are defined. The fifth line convert the 3×8 matrix of the nodal variables into a 1×24 vector \mathbf{p}_e which is related to the final size of the residual vector (1×24) and the tangent stiffness matrix (24×24), to be generated. The sixth line defines now the loop over all integration points used to integrate residual and tangent stiffness over the element volume. Due to the selected template ‘H1’ *AceGen* assumes that a Gauss point integration with $2 \times 2 \times 2$ point will be sufficient for the eight-noded brick.⁵ The in the seventh line the Gauss point coordinates Ξ applied in the integration loop are defined and in the last line the weight related to the Gauss point.

The shape functions of the eight-noded hexahedral element, see (74) are defined in the first four lines of Fig. 4. The fifth line computed in a very condensed way the coordinates \mathbf{X}_e and displacements \mathbf{u}_e in the element as given in (73). Furthermore in this line the Jacobi matrix \mathbf{J}_e , see (75), and its determinant are computed. In the sixth line the displacement gradient is computed using the chain rule provided in (75). The seventh line is the equivalent to (76), it computed deformation gradient \mathbf{F}_e , its determinant J_e and right Cauchy-Green tensor \mathbf{C}_e . In the sixth line the strain energy function, as given in (72) is defined. Once all this is done, the residual \mathbf{R} follows by

⁵The user can overrule the automatic selection of the integration rule, but this is only necessary when special shape functions are used.

Fig. 3 Basic definitions of material data, nodal values, and Gauss points and

```
{Em,v}+SMSReal[Table[es$$["Data",i},{i,2}]];
{λ,μ}+SMSHookeToLame[Em,v];
XIO=Table[SMSReal[nd$$[i,"X",j]},{i,nen},{j,ndim}];
uIO+SMSReal[Table[nd$$[i,"at",j]},{i,nen},{j,ndim}]];
pe=Flatten[uIO];
SMSDo[Ig,1,SMSInteger[es$$["id","NoIntPoints"]]];
Ξ={ξ,η,ζ}+Table[SMSReal[es$$["IntPoints",i,Ig]},{i,3}];
wgp+SMSReal[es$$["IntPoints",4,Ig]];
```

Fig. 4 Definition of shape functions, derivatives, and generation of residual and tangent matrix

```
Ξn={-1,-1,-1},{1,-1,-1},{1,1,-1},{-1,1,-1},{-1,-1,1},
{1,-1,1},{1,1,1},{-1,1,1}];
Nh=Table[1/8 (1+ξ Ξn[i,1]) (1+η Ξn[i,2]) (1+ζ Ξn[i,3]),
{i,1,nen}];
X+SMSFreeze[Nh.XIO];u=Nh.uIO;Je=SMSD[X,Ξ];Jed=Det[Je];
H=SMSD[u,X,"Dependency"→{Ξ,X,SMSInverse[Je]}];
F=IdentityMatrix[3]+H;Ce=F.F;JF=Det[F];
W=1/2 λ (JF-1)^2+μ (1/2 (Tr[Ce]-3)-Log[JF]);
Rg=Jed SMSD[W,pe];
Kg=SMSD[Rg,pe];
```

using differentiation of W with respect to the nodal displacements \mathbf{p}_e . This is done by the command 'SMSD.' Multiplication with the determinant of the Jacobian of the isoparametric transformation is necessary to obtain the correct volume integral in physical space of the element. Here, a different way is used to obtain the residual. The virtual work of the stresses in (48) can be written with the variation $\boldsymbol{\eta} = \delta \mathbf{u}$ by using the chain rule as

$$\mathbf{P} \cdot \text{Grad } \delta \mathbf{u} = \frac{\partial W}{\partial \mathbf{F}} \cdot \frac{\partial \mathbf{F}}{\partial \mathbf{u}} \delta \mathbf{u} = \frac{\partial W}{\partial \mathbf{u}} \cdot \delta \mathbf{u}. \quad (77)$$

Hence, the virtual work, see for the classical formulation (48), can now be redefined, leading to the residual is

$$\int_V \frac{\partial W}{\partial \mathbf{u}} \cdot \delta \mathbf{u} dV - \int_V \rho_0 (\bar{\mathbf{b}} - \dot{\mathbf{v}}) \cdot \delta \mathbf{u} dV - \int_{\partial V_\sigma} \bar{\mathbf{t}} \cdot \delta \mathbf{u} dA = 0. \quad (78)$$

The tangent matrix \mathbf{K}_T then simply follows from the derivative of the residual \mathbf{R} with respect to the nodal displacements \mathbf{p}_e .

The only operation that is left is the export of the symbolically generated residual and tangent matrix to a subroutine that can be called as user element in one of the finite element codes mentioned above. This is done as depicted in Fig. 5. The last statement closes the loop over the Gauss points, see Fig. 3.

Fig. 5 Code generation

```
SMSExport[wgp Rg,p$$,"AddIn"→True];
SMSExport[wgp Table[Kg[i,j]},{i,1,np},{j,i,np}],
Table[s$$[i,j]},{i,1,np},{j,i,np}], "AddIn"→True];
SMSEndDo[];
```

Formulation based on the weak form. Often it is not possible to develop finite elements starting from a strain energy function, e.g., in case of inelastic materials, and thus, the more general approach is to use the weak form. In that case, one can start from the weak form (50)

$$\int_V \mathbf{S}(\mathbf{u}) \cdot \frac{1}{2} \delta \mathbf{C} dV - \int_V \rho_0 \bar{\mathbf{b}} \cdot \delta \mathbf{u} dV - \int_{\partial V_\sigma} \bar{\mathbf{t}} \cdot \delta \mathbf{u} dA = 0. \quad (79)$$

where the second Piola–Kirchhoff stress tensor $\mathbf{S}(\mathbf{u})$ has to be expressed using a constitutive equation, $\mathbf{C}(\mathbf{u})$ is again the right Cauchy–Green tensor. The last two integrals are related to body and surface forces.

Now the isogeometric formulation with the same ansatz function as before is employed, and hence, Eqs. (73)–(76) are still valid. The only new equation that is needed is the stress response related to the strain energy defined in (72). This is obtained from

$$\mathbf{S} = 2 \frac{\partial W}{\partial \mathbf{C}} = \lambda J(J-1) \mathbf{C}^{-1} + \mu (\mathbf{1} - \mathbf{C}^{-1}). \quad (80)$$

Now the code included in Fig. 4 can be exchanged by the code depicted in Fig. 6. Here in the second line the Cauchy–Green tensor and its inverse are defined. Then in the next line the response function for the second Piola–Kirchhoff stress \mathbf{S} , see (80), is provided. After that follows a loop over all unknowns. Here, the variation of \mathbf{C} is computed in the fifth line by differentiation of the right Cauchy–Green tensor with respect to the displacement field. This is justified by

$$\delta \mathbf{C}_e(\mathbf{u}) = \delta \mathbf{C}_e(\mathbf{p}_e) = \frac{\partial \mathbf{C}_e}{\partial \mathbf{p}_e} \delta \mathbf{p}_e. \quad (81)$$

Note that $\delta \mathbf{p}_e$ is not needed in the formulation since it will be put in front of the residual vector, see, e.g., Wriggers (2008). The residual follows in the sixth line its form stems from the first integral in (79). Here, the last two integrals, defining the loading are omitted to have shorter code.

Fig. 6 Code generation using weak form

```
F=IdentityMatrix[3]+H;JF=Det[F];
Ct=FT.F;Cei=SMSInverse[Ct];
S=λ JF (JF-1) Cei+μ (IdentityMatrix[3]-Cei);
SMSDo[m,1,np];
δCt=SMSD[Ct,pe,m];
Rgm=Jed 1/2 Tr[δCt.S];
SMSEExport[wgp Rgm,pe,$m,"AddIn"→True];
SMSDo[n,m,np];
Kgm=SMSD[Rgm,pe,n];
SMSEExport[wgp Kgm,$m,$n,"AddIn"→True];
SMSEndDo[];
SMSEndDo[];
```

Fig. 7 Code generation using pseudo potential

```
Ct=FT.F;CeI=SMSInverse[Ct];
S=SMSFreeze[λ JF (JF-1) CeI+μ (IdentityMatrix[3]-CeI)];
WP=1/2 Tr[Ct.Transpose[S]];
SMSDo[m,1,np];
Rgm=Jed SMSD[WP,pe,m,"Constant"→S];
SMSEXP[wp Rgm,p$$[m],"AddIn"→True];
```

After that the standard procedure to export the code and to obtain the tangent stiffness matrix by differentiation of the residual with respect to the displacement field ends the formulation of the element based on the weak form.

Another possibility when using *AceGen* is to compute the residual in the following form

$$\mathbf{R} = \frac{J_e}{2} \mathbf{S}_e(\mathbf{p}_e) \cdot \frac{\partial \mathbf{C}_e(\mathbf{p}_e)}{\partial \mathbf{p}_e} = \frac{\partial W^P(\mathbf{p}_e)}{\partial \mathbf{p}_e} \Big|_{s_e=const.} \quad (82)$$

with the pseudo potential of the specific strain energy $W = \int_V \bar{W} dV$

$$\bar{W}^P(\mathbf{p}_e) = \frac{1}{2} \mathbf{S}_e(\mathbf{p}_e) \cdot \mathbf{C}_e(\mathbf{p}_e) = \frac{1}{2} \text{tr}[\mathbf{S}_e(\mathbf{p}_e)^T \mathbf{C}_e(\mathbf{p}_e)]. \quad (83)$$

Thus, the part that computes the residual in Fig. 6 can be exchanged with Fig. 7.

It is obvious that all formulations have to produce exactly the same results as the elements derived directly from the same strain energy. Here, the interesting question is: which of these formulations produces the more efficient code? Actually, it can be shown that the time to generate the code for the finite element is the shortest when the strain energy (72) is used. Using the weak form or the pseudo potential is 10–20 % slower. This also holds for the time to compute residual vector and tangent matrix since it takes about 70 % more time to evaluate the residual vector and tangent matrix.

Another observation is that the development of such element, once the basic structure of the toolbox is set, is very fast. The type of element, that is described in Fig. 4 only needs about 10–15 s to generate. Compared to the time one needs to write the code, and before, to derive residual, and tangent including debugging in all phases is a lot slower. Thus, it pays off to invest in understanding modern development software that can do derivations automatically like *AceGen*.

2.4 Mixed Elements for Incompressibility

Pure displacement elements tend to lock and thus will generate a too stiff response. In case of incompressible materials this phenomenon stems from the volumetric constraint $J = \det \mathbf{F} = 1$, and hence, is called volume locking. Mixed finite element methods can be introduced to avoid volume locking, see, e.g., Zienkiewicz and Taylor (1989) and Brezzi and Fortin (1991).

Finite elements that are derived from mixed methods have to fulfill additional mathematical conditions that guarantee the stability of the element formulation. For incompressibility this condition is known as BB-condition, named after its inventors Babuska and Brezzi, see e.g. Brezzi and Fortin (1991). A numerical method to investigate fulfillment of the BB-condition can be found in Chapelle and Bathe (1993). For general nonlinear applications there exists no direct formulation of the BB-condition, however, discussions in this direction can be found in Auricchio et al. (2013).

Different ways can be followed to construct mixed elements. Here, the specific strain energy is used to shorten notation.

Lagrangian multipliers The method of Lagrangian multipliers provides a classical way to enforce constraints. Here, as an example the incompressibility constraint $G(J) = J - 1 = 0$ (with $J = \det \mathbf{F}$) is considered which is directly introduced

$$\bar{W}(\mathbf{u}, p) = \bar{W}(\mathbf{C}(\mathbf{u})) + p G(J(\mathbf{u})). \quad (84)$$

The strain energy function $\bar{W}(\mathbf{C}(\mathbf{u}))$ is given by any of the functions defined in Sect. 1.3. In the finite element formulation occur now additional unknowns associated with the Lagrange multiplier p in addition to the displacements. In the case of incompressibility the Lagrange multiplier can be viewed as the pressure. Early finite element formulations that use this approach can be found in Oden and Key (1970) and Duffet and Reddy (1983).

Perturbed Lagrangian formulation This formulation is based on the following specific strain energy function

$$\bar{W}(\mathbf{u}, p) = \bar{W}(\mathbf{C}(\mathbf{u})) + p G(J(\mathbf{u})) - \frac{1}{2\epsilon} p^2. \quad (85)$$

The constraint condition is again given as in (84). $\epsilon > 0$ is a perturbation parameter. Choosing now continuous ansatz function for displacements and pressure. Due to the third term in (85) the pressures can be removed from the system. When discontinuous ansatz functions are used for the pressure p then they can be eliminated at element level and lead to a formulation that is equivalent to a *penalty* formulation.

Note that the solution now depends on the perturbation or penalty parameter. For small values of ϵ the influence of the constraint condition disappears. For large values of ϵ the constraint is fulfilled more and more exactly but the condition number of the equation system that appears in a Newton type solution will be very large. Many papers regarding various variants of (85) have been published. For the large strain case of rubber elasticity see, e.g., Haggblad and Sundberg (1983) and Sussman and Bathe (1987).

Hu–Washizu functional. In this functional the incompressibility constraint is formulated via a constitutive equation for the pressure, see (62). In short the specific strain energy

$$\bar{W}(\mathbf{u}, p, \theta) = \bar{W}(\hat{\mathbf{C}}(\mathbf{u})) + K [G(\theta)]^2 + p (J(\mathbf{u}) - \theta) \quad (86)$$

is formulated. Here ansatz functions can be selected for the displacement \mathbf{u} , the pressure p and the volumetric strain θ . $G(\theta)$ defines the constitutive equation for the pressure term, here K is the modulus of compression. The formulation of $W(\hat{\mathbf{C}})$ is provided by (39). A finite element based on this approach was firstly presented in Simo et al. (1985).

2.5 Mixed Element for Finite Deformations

The program *AceGen*, see Korelc (2011), is used now to generate finite elements for the cases discussed above.

Mixed element T2-P1 with Lagrangian multipliers In order to fulfill the equation for the volume constraint $J = 1$ exactly a pure mixed element is considered. It is based on a tetrahedral element with quadratic ansatz functions for the displacement field \mathbf{u} and linear ansatz functions for the pressure p . Since the most efficient formulation in *AceGen* is generated using the strain energy function. We can start from

$$W(\mathbf{u}, p) = \int_V \left\{ \frac{\mu}{2} [\text{tr} \mathbf{C}(\mathbf{u}) - 3] - \mu \log J(\mathbf{u}) + p [J(\mathbf{u}) - 1] \right\} dV \quad (87)$$

where the last term is related to the constraint. The mixed strain energy is closely related to the strain energy (72), only the first term in (72) is replaced by the third term in the strain energy in (87).

The mixed element has now to be generated using different ansatz functions for displacements and pressure. This can be achieved within *AceGen* in a way that is described in Fig. 8. The *SMSTemplate* defines the topology, here ‘O2’ means that a quadratic tetrahedra element is generated. It has 10 nodes and for the first 4 nodes 4 degrees of freedom (displacement and pressure variables) and the last 6 nodes 3 degrees of freedom (displacement variables). This is also denoted by the *SMSNodeID* where ‘Mix -L’ stands for pressure and displacements and ‘D’ for displacements. Coordinates of the nodes are defined as usual. However, the unknown nodal values are contained in a table from which one has to extract the displacement and pressure unknowns. This is done in line 10 of Fig. 8.

Additionally a body force is defined in 12 and 13 where q is the load vector and ‘mult’ the load factor.

After this definition of the general element quantities the isoparametric ansatz and the physical problem can be described. In Fig. 9 the first three lines define the loop

```

SMSInitialize["T2-P1-3d", "Environment" → "AceFEM", "Mode" → "Optimal"];
SMSTemplate[
  "SMSTopology" → "Q2", "SMSNoNodes" → 10, "SMSDOFGlobal" → {4, 4, 4, 4, 3, 3, 3, 3, 3, 3},
  "SMSNodeID" → {"MIX -L", "MIX -L", "MIX -L", "MIX -L", "D", "D", "D", "D", "D", "D"},
  "SMSDomainDataNames" → {"μ", "Qx", "Qy", "Qz"},
  "SMSDefaultData" → {42, 0, 0, 0}, "SMSSymmetricTangent" → True]
SMSStandardModule["Tangent and residual"];
nen = SMSNoNodes; ndim = SMSNoDimensions; np = SMSNoDOFGlobal;
XIO = Table[SMSReal[nd$$[{i, "x", j}], {i, nen}, {j, ndim}];
peIO = SMSReal[Table[nd$$[{i, "at", j}], {i, nen}, {j, SMSDOFGlobal[[i]]}]];
pe = Flatten[peIO];
uIO = peIO[[{1, 2, 3, 4, 5, 6, 7, 8, 9, 10}], {1, 2, 3}]; pIO = peIO[[{1, 2, 3, 4}], 4];
{μ, Qx, Qy, Qz} = SMSReal[Table[es$$["Data", i], {i, 4}]];
q = {Qx, Qy, Qz};
mult = SMSReal[rdata$$["Multiplier"]];

```

Fig. 8 First part of *AceGen* code for a mixed element

```

SMSDo[Ig, 1, SMSInteger[es$$["id", "NoIntPoints"]]];
Σ = {ξ, η, ζ} = Table[SMSReal[es$$["IntPoints", i, Ig]], {i, 3}];
wgp = SMSReal[es$$["IntPoints", 4, Ig]];
κ = 1 - ξ - η - ζ;
Nh = {(2ξ - 1)ξ, (2η - 1)η, (2ζ - 1)ζ, (2κ - 1)κ, 4ξη, 4ηζ, 4ξζ, 4ξκ, 4ηκ, 4ζκ};
Np = {ξ, η, ζ, κ};
X = SMSFreeze[Nh.XIO]; u = Nh.uIO; p = Np.pIO;
Je = SMSD[X, Σ]; Jed = Det[Je];
H = SMSD[u, X, "Dependency" → {Σ, X, SMSInverse[Je]}];
F = IdentityMatrix[3] + H;
Ct = FT.F; JF = Det[F];
W = μ  $\frac{1}{2}$  (Tr[Ct] - 3) - μ Log[JF] + p (JF - 1) - mult q.u;

```

Fig. 9 Second part of *AceGen* code for a mixed element

over the Gauss points, the isoparametric coordinates and the weighting factors related to the Gauss points within the numerical integration procedure. The fourth to fifth line defines the quadratic shape functions ‘Nh’ for the displacement interpolation

$$\begin{aligned}
N_1 &= (2\xi - 1)\xi, \quad N_2 = (2\eta - 1)\eta, \quad N_3 = (2\zeta - 1)\zeta, \quad N_4 = (2\kappa - 1)\kappa, \\
N_5 &= 4\xi\eta, \quad N_6 = 4\eta\zeta, \quad N_7 = 4\xi\zeta, \quad N_8 = 4\xi\kappa, \quad N_9 = 4\eta\kappa, \quad N_{10} = 4\zeta\kappa,
\end{aligned}$$

with $\kappa = 1 - \xi - \eta - \zeta$. Furthermore, in the sixth line, the linear shape functions ‘Np’ are defined

$$Np_1 = \xi, \quad Np_2 = \eta, \quad Np_3 = \zeta, \quad Np_4 = \kappa$$

that will be used to interpolate the pressure variables within the element. The ansatz for u and p is defined in the seventh line of Fig. 9. The next line describes the derivation of the Jacobi matrix that defines the isoparametric map. After that the displacement, \mathbf{H} , and the deformation gradient \mathbf{F} , see (8), are computed as well as the right Cauchy-Green tensor \mathbf{C} and the determinant J of \mathbf{F} . For more details, see also the description in Fig. 4. These kinematic variables are needed to define the specific strain energy \bar{W} in the last line of Fig. 9.

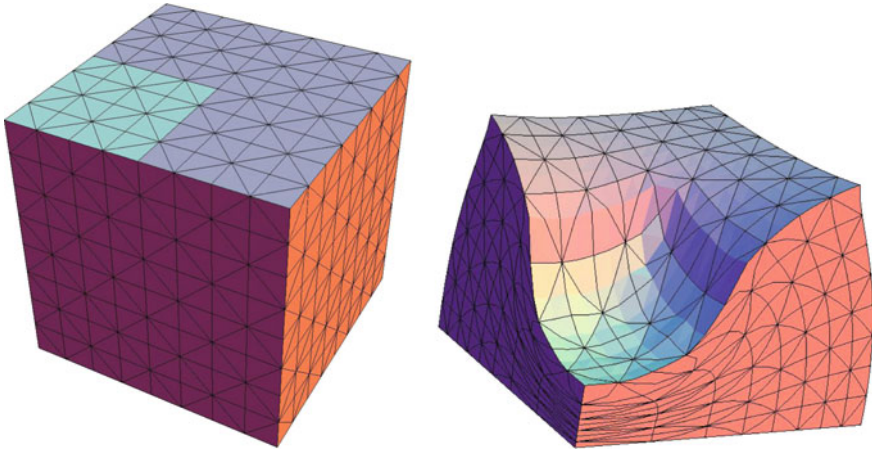


Fig. 10 Undeformed and severely deformed configuration of a block (a quarter of the mesh)

The residual and tangent matrix follows then by the same procedure that is provided in Fig. 4. No difference has been made with respect to displacement and pressure variables, since these are combined in the vector \mathbf{p}_e and the command `MSD` differentiates the strain energy function with respect to all variables and thus will produce the full residual vector that has the length of the 34 unknowns. Thus, the tangent matrix has the size 34×34 where zero elements appear on the diagonal related to the pressure degree of freedom. Thus special equation solvers have to be used to solve engineering problems in a reliable way.

As an example to highlight the performance of the mixed element a block which is partly loaded by a constant surface load is considered. Figure 10 depicts a quarter of a mesh and deformed configuration of a block of rubber-like material. The block is discretized using the mixed T2-P1 element described above. The block has dimensions of $100 \times 100 \times 50$.⁶ It is on rollers at the bottom. Furthermore symmetry conditions are applied to be able to compute only one quarter of the block. Furthermore, the displacements at the top of the block are fixed in X and Y direction. The block is, as shown in Fig. 10, discretized by $8 \times 8 \times 8$ T2-P1 elements. This leads to a total of 2592 elements and 12521 unknowns. Material data need only be provided for the shear modulus it is selected as $\mu = 1.61148$. A surface load of $q = 9$ is applied at the part that is colored in turquoise in three load steps.

This loading leads to a severely deformed configuration. Newton's method is applied to solve the problem. It should be noted that the solution within each load step converges quadratically. The element depicts a very robust behavior since only three load steps, and within each load step only six iterations were needed to converge.

⁶All data are provided as dimensionless constants, it is assumed that the dimensions match real physical data.

Table 1 Convergence of the mid-displacement using the T2-P1 element

Mesh division	d.o.f	u_z	Total iterations
$2 \times 2 \times 2$	263	-30,803	19
$4 \times 4 \times 4$	1733	-38,344	19
$8 \times 8 \times 8$	12521	-39,271	18
$16 \times 16 \times 16$	95057	-39,349	18
$24 \times 24 \times 16$	315193	-39,372	18

The convergence behavior of the maximal displacement in vertical direction for the final load of $q = 9$ is depicted in Table 1 for a variety of discretizations.

Thus, the mixed element is efficient and robust and applicable for finite strain cases with severe deformations.

Mixed element Q1-P0 based on Hu–Washizu’s principle In this section, we derive a large deformation finite element which is based on the Hu–Washizu variational formulation. This element, developed in Simo et al. (1985), is implemented in many existing finite element codes and uses linear shape functions for the deformation field related to the deviatoric kinematical variables. The shape functions for the displacements are the same as in (74). The mixed/enhanced variables, pressure p , and volumetric strain θ , are approximated by shape functions that are assumed to be constant.

The formulation starts from the special Hu–Washizu principle (62). Here, the specific strain energy \bar{W} is given as

$$\bar{W}(\mathbf{u}, p, \theta) = \frac{\mu}{2} \left(J^{-\frac{2}{3}} \text{tr} \mathbf{C} - 3 \right) + p \left[J - \frac{J_e}{J_{e0}} \theta \right] + \frac{K}{2} \left[\frac{J_e}{J_{e0}} \theta - 1 \right]^2. \quad (88)$$

Here $J_e = \det \mathbf{J}_e$ is the determinant of Jacobi matrix of the isoparametric transformation and $J_{e0} = \det \mathbf{J}_{e0}$ is the same determinant evaluated at the element center. This special form of \bar{W} was selected in order to obtain the same element formulation as provided in Simo et al. (1985) in which the integrals for the mixed parts are evaluated differently using one point integration.

In this formulation the two additional unknowns p and θ can be eliminated at element level by using the Schur complement. This is automatically done in *AceGen* when variables are defined by the “SMSNoDOFCondense” command in the template, see Fig. 11. The associated variables are defined in the 10th line of the input and are combined with the displacement variables to the general unknown vector in line 11. All the rest is standard input where “H1” in the second line defines the topology of the 8 noded hexahedral element.

The second part of the *AceGen* input for the Q1-P0 element is provided in Fig. 12. The shape function for the element are defined in lines 4 and 5. Then the standard procedure as before leads to the displacement interpolation in the element. New is the computation of $\det \mathbf{J}_{e0}$ in line 9 and the definition of the mixed variables p and

```

SMSInitialize["Q1P0", "Environment" → "AceFEM", "Mode" → "Optimal"];
SMSTemplate["SMSTopology" → "H1"
, "SMSNoDOFCondense" → 2
, "SMSDomainDataNames" → {"x", "μ", "Qx", "Qy", "Qz"}
, "SMSDefaultData" → {501, 1.61148, 0, 0, 0}];
SMSStandardModule["Tangent and residual"];
nen = SMSNoNodes; ndim = SMSNoDimensions; np = SMSNoDOFGlobal; nhe = SMSNoDOFCondense;
XIO = Table[SMSReal[nd$[i, "x", j]], {i, nen}, {j, ndim}];
peIO = SMSReal[Table[nd$[i, "at", j], {i, nen}, {j, SMSDOFGlobal[[i]]}];
heIO = SMSReal[Array[ed$[i, "ht", #] & nhe];
pe = Flatten[{peIO, heIO}];
{κ, μ, Qx, Qy, Qz} = SMSReal[Array[es$[i, "Data", #1] & 5];
q = {Qx, Qy, Qz};
mult = SMSReal[rdata$[i, "Multiplier"];

```

Fig. 11 First part of *AceGen* code for the Q1-P0 element based on the Hu–Washizu principle

```

SMSDo[Ig, 1, SMSInteger[es$[i, "id", "NoIntPoints"]];
E = {ξ, η, ζ} = Table[SMSReal[es$[i, "IntPoints", i, Ig]], {i, 3}];
wgp = SMSReal[es$[i, "IntPoints", 4, Ig]];
{ξ1, η1, ζ1} = {{-1, 1, 1, -1, -1, 1, 1, -1}, {-1, -1, 1, 1, -1, -1, 1, 1}, {-1, -1, -1, -1, 1, 1, 1, 1}};
Nh = MapThread[1/8 (1 + ξ #1) (1 + η #2) (1 + ζ #3) &, {ξ1, η1, ζ1}];
X = SMSFreeze[Nh.XIO]; u = Nh.peIO;
Je = SMSD[X, E]; Jed = Det[Je];
H = SMSD[u, X, "Dependency" → {E, X, SMSInverse[Je]}];
Je0 = SMSReplaceAll[Je, {ξ → 0, η → 0, ζ → 0}]; J0 = Det[Je0];
θ = heIO[[1]] + 1; p = heIO[[2]];
F = IdentityMatrix[3] + H;
JF = Det[F]; Ct = F'.F;
W = p (JF - θ J0 / Jed) + μ / 2 (JF ^ (-2/3) Tr[Ct] - 3) + κ / 2 (θ J0 / Jed - 1) ^ 2 - mult q.u;
SMSDo[m, 1, np + nhe];
Rgm = Jed SMSD[W, pe, m];
SMSEXP[wp, Rgm, p$[m], "AddIn" → True];
SMSDo[n, m, np + nhe];
Kgm = SMSD[Rgm, pe, n];
SMSEXP[wp, Kgm, s$[m, n], "AddIn" → True];
SMSEndDo[];
SMSEndDo[];
SMSEndDo[];
SMSWrite[];

```

Fig. 12 Second part of *AceGen* code for the Q1-P0 element based on the Hu–Washizu principle

θ in line 10. Note that the constant 1 is added to θ in order to obtain a zero energy state in the initial configuration. After that all is standard. One only has to take care that the loops now run over all displacements and the mixed variables, see line 14 and 17.

The same example of the block under surface load, as in the section before, is computed to depict the efficiency and robustness of this element formulation. The mesh and deformed mesh of a discretization with $32 \times 32 \times 32$ elements for an applied load of $q = 9$ is shown in Fig. 13. This again depicts the finite deformation state under the given load.

The convergence behavior of the maximal displacement when using the Q1-P0 element in vertical direction for the final load of $q = 9$ is depicted in Table 2 for a variety of discretizations. It can be seen that contrary to the T2-P1 element this Q1-P0 formulation converges in a different way. Small numbers of elements yield a solution that is too weak. However, both formulations converge to the same value.

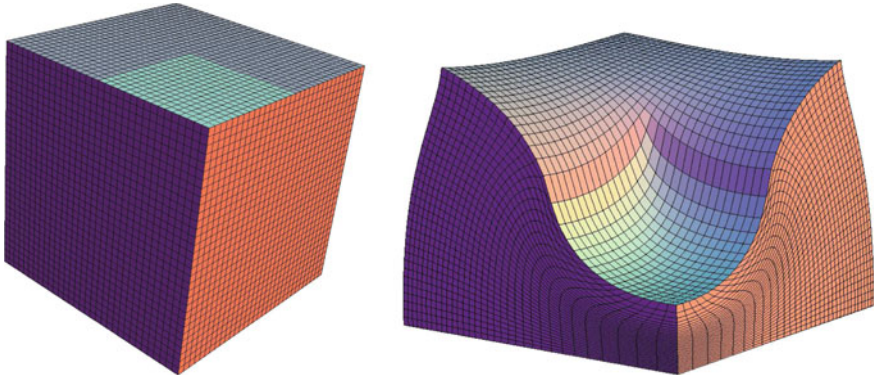


Fig. 13 Undeformed and severely deformed configuration of a block (a quarter of the mesh)

Table 2 Convergence of the mid-displacement using the Q1-P0 element

Mesh division	d.o.f	u_z	Total iterations
$2 \times 2 \times 4$	42	-45,085	18
$4 \times 4 \times 4$	260	-41,324	20
$8 \times 8 \times 8$	1800	-40,562	20
$16 \times 16 \times 16$	13328	-39,675	20
$32 \times 32 \times 32$	102432	-39,463	20
$48 \times 48 \times 32$	341040	-39,425	20

Mixed element for anisotropic material The last example is concerned with a three-dimensional finite element for anisotropic material behavior at finite strains. In this example the formulation accounts for transversely isotropic material behavior by using a mixed approach. It is assumed that the material is not extendable in the given direction \mathbf{a} .

The isotropic strain energy function W^{iso} which describes the behavior of the isotropic part of the material is given by

$$W^{iso}(\mathbf{u}) = \frac{\mu}{2}(\text{tr } \mathbf{C} - 3 - 2 \log J) + \frac{\lambda}{4}(J^2 - 1 - 2 \log J) \quad (89)$$

where μ and λ are the Lamé constants. The enforcement of the constraint that ensures that the material does not extend in the direction of \mathbf{a} leads to the following condition

$$\mathbf{a} \cdot \mathbf{E} \mathbf{a} = 0 \quad (90)$$

where \mathbf{E} is the Green-Lagrangian strain tensor, see (9). Since it is simpler to work with the right Cauchy-Green tensor \mathbf{C} this constraint can be written as

$$\mathbf{a} \cdot \mathbf{E} \mathbf{a} = \mathbf{a} \cdot (\mathbf{C} - \mathbf{1}) \mathbf{a} = \mathbf{a} \cdot \mathbf{C} \mathbf{a} - 1 \quad \text{for } \|\mathbf{a}\| = 1. \quad (91)$$

Furthermore we can write

$$\mathbf{a} \cdot \mathbf{C} \mathbf{a} = \mathbf{C} \cdot \mathbf{M} = \text{tr}[\mathbf{C} \mathbf{M}] \quad \text{with } \mathbf{M} = \mathbf{a} \otimes \mathbf{a}. \quad (92)$$

Thus, the Lagrange multiplier term related to the constraint of a material that is not extendable in the direction \mathbf{a} yields

$$W^{ti}(\mathbf{u}, p) = p (\text{tr}[\mathbf{C} \mathbf{M}] - 1) \quad (93)$$

which then leads to the final form of the strain energy

$$W(\mathbf{u}, p) = W^{iso}(\mathbf{u}) + W^{ti}(\mathbf{u}, p). \quad (94)$$

A tetraeder element with quadratic interpolation for the displacement field \mathbf{u} and linear interpolation for the mixed variable p is selected.⁷ Thus, the same shape functions as for the first element, T2-P1, in Sect. 2.5 can be used which leads to an *AceGen* input that is equivalent for the first part with the code depicted in Fig. 8. The only difference is that the vector \mathbf{a} defining the direction of the anisotropy has to be defined as element input as $\mathbf{a} = \{a_x, a_y, a_z\}$.

The second part of the code is shown in Fig. 14. Again the shape functions for the displacement and the mixed variable are defined as well as the kinematical relations. New in this formulation is the computation of the structure tensor \mathbf{M} , see (92), and the tensor product $\mathbf{C} \mathbf{M}$. After that the strain energy can be formulated. It is given in the last line of the input. The first two terms are related to the isotropic part W^{iso} while the last term defines the Lagrange multiplier term, W^{ti} , including the constraint (91).

An example that will show a clear anisotropic response is the Cook's membrane problem of a tapered cantilever, clamped at the left end. The structure is loaded at the right end by a constant vertical load, as depicted in left part of Fig. 15. The selected data for the Lamé constants are $\mu = 500$ and $\lambda = 1000$. The direction of anisotropy is given by $\mathbf{a} = \frac{1}{\sqrt{3}}\{1, 1, 1\}$.

Different mesh densities were used to compute the solution. The deformed mesh in Fig. 15 was computed with a mesh of $16 \times 16 \times 4$ elements which lead to a total number of 26885 degree of freedoms. The deformation clearly depicts the twist in the deformed shape due to the anisotropic constraint at large deformations. The solution was computed with several load steps. In total 10 load steps were applied for all discretizations reported in Table 3. The convergence behavior was robust, six iterations per load step were needed for all discretizations to obtain convergence. In this solution, procedure Newton type convergence was observed.

Table 3 shows the convergence behavior of the end displacement at the top node ($X = 48, Y = 60, Z = 0$) for the Z -displacement u_{zu} and the Y -displacement u_y . Furthermore the displacement u_{zb} at the node ($X = 48, Y = 44, Z = 0$) is reported to depict the torsion of the cross section.

⁷Here the variable p is the stress component related to the constraint, e.g., the stress in direction of \mathbf{a} . It has to be scaled in order to yield the correct stress.

```

SMSDo[Ig, 1, SMSInteger[es$$["id", "NoIntPoints"]]];
E = {ξ, η, ζ} ⊢ Table[SMSReal[es$$["IntPoints", i, Ig]], {i, 3}];
wgp ⊢ SMSReal[es$$["IntPoints", 4, Ig]];
κ = 1 - ξ - η - ζ;
Nh = {(2 ξ - 1) ξ, (2 η - 1) η, (2 ζ - 1) ζ,
      (2 κ - 1) κ, 4 ξ η, 4 η ζ, 4 ξ ζ, 4 ξ κ, 4 η κ, 4 ζ κ};
Np = {ξ, η, ζ, κ};
X ⊢ SMSFreeze[Nh.XIO];
u = Nh.uIO; p = Np.pIO;
Je = SMSD[X, E]; Jed = Det[Je];
H = SMSD[u, X, "Dependency" → {E, X, SMSInverse[Je]}];
F = IdentityMatrix[3] + H;
Ct = FT.F; JF = Det[F];
a = {ax, ay, az};
M = Outer[Times, a, a];
CM = Ct.M;
W = μ  $\frac{1}{2}$  (Tr[Ct] - 3 - 2 Log[JF]) + λ / 4 (JF2 - 1 - 2 Log[JF]) + (Tr[CM] - 1) p;

```

Fig. 14 Second part of *AceGen* code for the mixed element with transversely anisotropic material

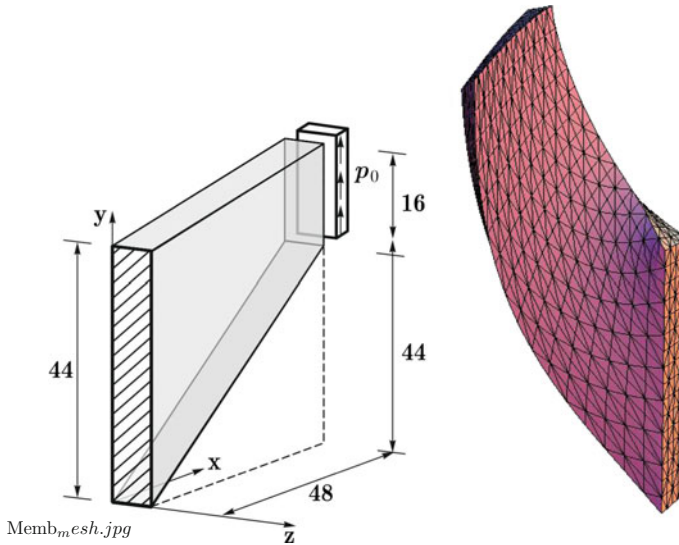


Fig. 15 Undeformed and severely deformed configuration of a block (a quarter of the mesh)

Note that the convergence is not completely monotonic. This results from the fact that the mesh density in Z-direction was kept constant. This choice would not make a difference in the isotropic case, however, due to anisotropic material behavior the cantilever deforms in all directions, and thus, the discretization also in Z-direction plays a role.

Table 3 Convergence of the end displacements using the T2-P1 element for an anisotropic material

Mesh division	d.o.f	u_y	u_{zu}	u_{zb}
$2 \times 2 \times 4$	537	19,859	-1,1639	-7,6436
$4 \times 4 \times 4$	1877	21,684	-0,3660	-8,5128
$8 \times 8 \times 4$	6981	21,966	-0,2167	-8,8043
$16 \times 16 \times 4$	26885	22,009	-0,2303	-8,8332
$32 \times 32 \times 4$	105477	22,021	-0,2326	-8,8186

3 Conclusions

Finite element development has to be based on rigorous continuum mechanics. This is necessary in order to treat finite strain cases correctly and to be able to investigate the best formulations for efficient and robust numerical solution schemes. With a general automated approach, like the methodology provided in *AceGen* it is possible to explore many different but theoretically equivalent continuum formulations in order to find the most efficient discretization scheme.

This contribution was focussed on both aspects. Due to limited space not all continuum formulations were discussed in the light of the associated finite element formulations. However several—even non standard aspects—like the introduction of pseudo potential formulations were discussed in the light of efficient and simple formulations for the development of finite elements.

This contribution has focused on elastic materials, but the same ideas can also be applied to inelastic material response. An in depth discussion of the related theoretical and numerical framework would have been too extensive and thus could not be covered. This is left for future discussions.

References

- Altenbach, J., & Altenbach, H. (1994). *Einführung in die Kontinuumsmechanik*. Stuttgart: Teubner-Verlag.
- Arnold, D. N., Brezzi, F., & Douglas, J. (1984). Peers: A new mixed finite element for plane elasticity. *Japan Journal of Applied Mathematics*, 1, 347–367.
- Auricchio, F., da Veiga, L. B., Lovadina, C., Reali, A., Taylor, R. L., & Wriggers, P. (2013). Approximation of incompressible large deformation elastic problems: some unresolved issues. *Computational Mechanics*, 52, 1153–1167.
- Becker, E., & Bürger, W. (1975). *Kontinuumsmechanik*. Stuttgart: B.G. Teubner.
- Belytschko, T., Ong, J. S. J., Liu, W. K., & Kennedy, J. M. (1984). Hourglass control in linear and nonlinear problems. *Computer Methods in Applied Mechanics and Engineering*, 43, 251–276.
- Braess, D. (1992). *Finite elemente*. Berlin: Springer.
- Brezzi, F., & Fortin, M. (1991). *Mixed and hybrid finite element methods*. Berlin: Springer.
- Chadwick, P. (1999). *Continuum mechanics, Concise theory and problems*. Mineola: Dover Publications.

- Chapelle, D., & Bathe, K. J. (1993). The inf-sup test. *Computers and Structures*, 47, 537–545.
- Ciarlet, P. G. (1988). *Mathematical elasticity I: Three-dimensional elasticity*. Amsterdam: North-Holland.
- Cottrell, J. A., Hughes, T. J. R., & Bazilevs, Y. (2009). *Isogeometric analysis: Toward integration of CAD and FEA*. New York: Wiley.
- Duffet, G., & Reddy, B. D. (1983). The analysis of incompressible hyperelastic bodies by the finite element method. *Computer Methods in Applied Mechanics and Engineering*, 41, 105–120.
- Eringen, A. (1967). *Mechanics of Continua*. New York: Wiley.
- Flory, P. (1961). Thermodynamic relations for high elastic materials. *Transactions of the Faraday Society*, 57, 829–838.
- Fraeijs de Veubeke, B. M. (1975). Stress function approach. In *World Congress on the Finite Element Method in Structural Mechanics* (pp. 1–51). Bournemouth.
- Häggblad, B., & Sundberg, J. A. (1983). Large strain solutions of rubber components. *Computers and Structures*, 17, 835–843.
- Holzappel, G. A. (2000). *Nonlinear solid mechanics*. Chichester: Wiley.
- Hughes, T. R. J. (1987). *The finite element method*. Englewood Cliffs: Prentice Hall.
- Korelc, J. (1997). Automatic generation of finite-element code by simultaneous optimization of expressions. *Theoretical Computer Science*, 187, 231–248.
- Korelc, J. (2002). Multi-language and multi-environment generation of nonlinear finite element codes. *Engineering with Computers*, 18, 312–327.
- Korelc, J. (2011). *AceGen and AceFEM user manual*. Technical report. University of Ljubljana. <http://www.fgg.uni-lj.si/symech/>.
- Malvern, L. E. (1969). *Introduction to the mechanics of a continuous medium*. Englewood Cliffs: Prentice-Hall.
- Marsden, J. E., & Hughes, T. J. R. (1983). *Mathematical foundations of elasticity*. Englewood Cliffs: Prentice-Hall.
- Mathematica. (2011). <http://www.wolfram.com>.
- Oden, J. T., & Key, J. E. (1970). Numerical analysis of finite axisymmetrical deformations of incompressible elastic solids of revolution. *International Journal of Solids and Structures*, 6, 497–518.
- Ogden, R. W. (1984). *Non-linear elastic deformations*. Chichester: Ellis Horwood and Wiley.
- Reese, S. (2005). On a physically stabilized one point finite element formulation for three-dimensional finite elasto-plasticity. *Computer Methods in Applied Mechanics and Engineering*, 194, 4685–4715.
- Reese, S., & Wriggers, P. (2000). A new stabilization concept for finite elements in large deformation problems. *International Journal for Numerical Methods in Engineering*, 48, 79–110.
- Simo, J. C., & Armero, F. (1992). Geometrically non-linear enhanced strain mixed methods and the method of incompatible modes. *International Journal for Numerical Methods in Engineering*, 33, 1413–1449.
- Simo, J. C., Armero, F., & Taylor, R. L. (1993). Improved versions of assumed enhanced strain tri-linear elements for 3D finite deformation problems. *Computer Methods in Applied Mechanics and Engineering*, 110, 359–386.
- Simo, J. C., & Rifai, M. S. (1990). A class of assumed strain methods and the method of incompatible modes. *International Journal for Numerical Methods in Engineering*, 29, 1595–1638.
- Simo, J. C., Taylor, R. L., & Pister, K. S. (1985). Variational and projection methods for the volume constraint in finite deformation elasto-plasticity. *Computer Methods in Applied Mechanics and Engineering*, 51, 177–208.
- Stenberg, R. (1988). A family of mixed finite elements for elasticity problems. *Numerische Mathematik*, 48, 513–538.
- Sussman, T., & Bathe, K. J. (1987). A finite element formulation for nonlinear incompressible elastic and inelastic analysis. *Computers and Structures*, 26, 357–409.
- Taylor, R. L. (2011). *FEAP: A finite element analysis program*. Technical report. <http://www.ce.berkeley.edu/feap>.

- Truesdell, C., & Noll, W. (1965). The nonlinear field theories of mechanics. In S. Flügge (Ed.), *Handbuch der Physik III/3*. Berlin: Springer.
- Truesdell, C., & Toupin, R. (1960). The classical field theory. *Handbuch der Physik III/1*. Berlin: Springer.
- Washizu, K. (1975). *Variational methods in elasticity and plasticity* (2nd ed.). Oxford: Pergamon Press.
- Wriggers, P. (2008). *Nonlinear finite elements*. Berlin: Springer.
- Zienkiewicz, O. C., & Taylor, R. L. (1989). *The finite element method* (4th ed., Vol. 1). London: McGraw Hill.
- Zienkiewicz, O. C., & Taylor, R. L. (2000). *The finite element method* (5th ed., Vol. 2). Oxford: Butterworth-Heinemann.
- Zienkiewicz, O. C., Taylor, R. L., & Too, J. M. (1971). Reduced integration technique in general analysis of plates and shells. *International Journal for Numerical Methods in Engineering*, 3, 275–290.

Advanced Finite Element Technologies

Schröder, J.; Wriggers, P. (Eds.)

2016, VII, 236 p. 92 illus., 47 illus. in color., Hardcover

ISBN: 978-3-319-31923-0